New Journal of Physics
The open access journal at the forefront of physics
Deutsche Physikalische Gesellschaft DPG | IOP Institute of Physics

Broadband and broadangle extraordinary acoustic transmission through subwavelength apertures surrounded by fluids

S Carretero-Palacios[1], A R J Murray[2], L Martín-Moreno[1] and A P Hibbins[2]

[1] Instituto de Ciencia de Materiales de Aragón and Departamento de Física de la Materia Condensada, CSIC-Universidad de Zaragoza, E-50009 Zaragoza, Spain
[2] Electromagnetic and Acoustic Materials Group, Department of Physics and Astronomy, University of Exeter, Stocker Road, Exeter EX4 4QL, UK
E-mail: sol.carretero@csic.es

Received 1 June 2014
Accepted for publication 17 July 2014
Published 27 August 2014

New Journal of Physics **16** (2014) 083044

doi:10.1088/1367-2630/16/8/083044

Abstract

We present a mechanism for ultra-broadband transmission of acoustic waves through subwavelength hole arrays. Different fluids surrounding (or filling) the holes are considered, which allows tuning of the band of maximum transmission to different angles of incidence. For certain configurations, this band of total transmission may appear at very small incident angles, making the system 'invisible' to sound at almost normal incidence. Analytical expressions for the specific incident angle, and for maximum transmission at that angle, are provided for any fluid-system configuration.

Keywords: surface waves, subwavelength apertures, extraordinary acoustic transmission

1. Introduction

Since the discovery of the resonant phenomenon of extraordinary optical transmission [1, 2], the study of electromagnetic (EM) waves propagating through subwavelength hole arrays has attracted much attention. This discovery was subsequently transferred to acoustic waves [3–6], despite the differences between the vector EM and scalar acoustic cases. Recently, a non-

Content from this work may be used under the terms of the Creative Commons Attribution 3.0 licence. Any further distribution of this work must maintain attribution to the author(s) and the title of the work, journal citation and DOI.

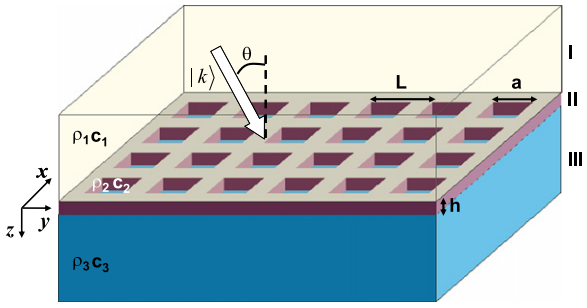

Figure 1. Diagram of a 2D hole array of period L in a screen of thickness h, perforated with square holes of side a. Different fluids in regions I, II and III, characterized by a density and speed of sound (ρ_1, c_1), (ρ_2, c_2), and (ρ_3, c_3), respectively, are considered. The angle of incidence with respect to the normal is θ.

resonant mechanism providing total transmission over ultrabroad bandwidths at specific incident angles (referred as 'plasmonic Brewster angles') has been reported for EM waves [7], and equivalently, for acoustic ones [8–11]. Both cases are impedance matching phenomena, and this condition is only provided for symmetric configurations where the same medium at the incident and transmission regions are considered.

In this paper we study theoretically the transmission of acoustic waves through subwavelength apertures in the general case when different fluids fill the reflection and transmission semi-infinite spaces, and also the apertures themselves. We provide analytical expressions for the angle and for the transmittance on this condition, which we show depend on the hole size, array period, L, and fluids properties (their density, ρ, and speed of sound, c), but not on the film thickness, h, as this is an impedance matching phenomenon. We obtain broadband transmission not only in frequency but also in incident angles close to normal incidence.

2. Resonant Brewster-like angle

2.1. Homogeneous system ($c_1 = c_2 = c_3$ and $\rho_1 = \rho_2 = \rho_3$)

Consider the schematic in figure 1: a perfectly rigid (PR) screen of thickness h, perforated with two-dimensional (2D) holes periodically arranged in a square lattice (with period L). The shape of the holes does not strongly influence the impedance matching condition, being mainly dependent on hole area, A. In this paper we consider either squares of side a, or circles of radius r, and we investigate the effect in transmission when different fluids are considered. The PR approximation, in which the externally applied energy vanishes inside the rigid body and transmission through the plates themselves is neglected, is an excellent approach to treat stiff materials, like steel or brass [12], when they are in proximity to flexible materials or air. The theoretical formalism used throughout this paper is based on this PR approximation and it consists of a modal expansion of the pressure and velocity fields in the different regions. Waves are expanded into Bloch modes in the reflection (I) and transmission (III) regions (characterized by (ρ_1, c_1) and (ρ_3, c_3), respectively), and the field inside the holes (characterized by (ρ_2, c_2)) is written as a linear combination of the eigenmodes. Imposing the appropriate matching conditions at the interfaces (I–II and II–III), only the amplitudes of the z-component of the

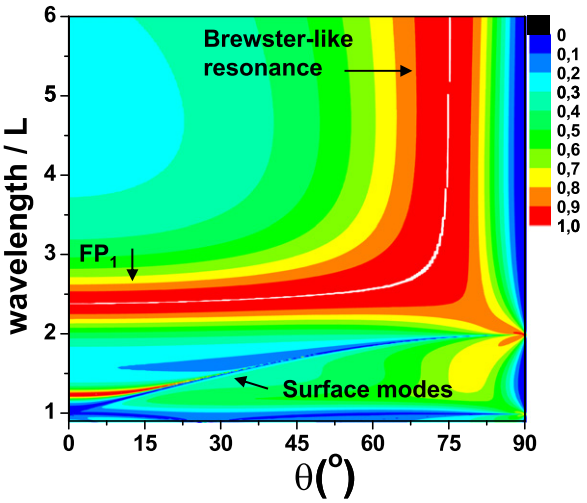

Figure 2. Angular transmission spectra for an array with square holes with $a/L = 0.53$, $h/L = 1.0$, $\rho_1 = \rho_2 = \rho_3$ and $c_1 = c_2 = c_3$. In this case, $\theta_B = 76.7°$, depicted with a dashed vertical line.

velocity field at the entrance (v) and exit (v') sides of the cavities must be computed to obtain an entire field mapping comprising far field and near field distributions. Transmission is then defined as

$$T = \frac{G_i^{III}}{Z_{k^0}^{I}} \left| \frac{I_0 G_\nu}{\left(G^{I} - \Sigma\right)\left(G^{III} - \Sigma\right) - G_\nu^2} \right|^2, \tag{1}$$

where I_0 measures the overlap between the incident plane wave and the fundamental mode inside the hole, Σ represents the bouncing back and forth of the acoustic waves inside the cavities, and the term G_ν is linked to the coupling between the two sides of the screen through the holes. Finally, $G^{I,\,III}$ account for the acoustic coupling between the fundamental eigenmode and all the diffractive waves (in regions I and III, respectively). Analytical expressions for all these quantities are defined in the appendix.

Figure 2 shows the angular transmission spectra for the simplest case of an homogeneous system (i.e., $c_1 = c_2 = c_3$ and $\rho_1 = \rho_2 = \rho_3$). In this calculation, we consider an array with square holes of side $a/L = 0.53$, and thickness $h/L = 1.0$. This set of geometrical parameters clearly shows three types of transmission mechanisms associated with these systems: that associated with surface modes at $\lambda \geqslant L \cdot (1 + \sin(\theta))$, which depends on both the incident wavelength in region I (λ) and angle (θ); Fabry–Pérot (FP) resonances at wavelengths close to $\lambda = 2h/l$ (with $l = 1, 2, ...$), which do not depend on the incident angle; and finally, an ultrabroadband resonance of total transmission, $T = 1$, at a given Brewster-like angle $\theta_B = 76.7°$, which does not depend on either the incident wavelength (for $\lambda \leqslant 2h$) or film thickness. As it has been previously demonstrated, these phenomena are achieved under some form of resonant condition [4], or when the system is anomalously impedance matched [8–10] at $\cos(\theta_B) = F$, with $F = A/L^2$ the 'filling factor' of a unit cell. Clearly, for homogeneous systems, the tunability of the ultrabroadband resonance to small incident angles is limited by the geometry of the system. However, in the following, we will show that the incorporation of

different fluids filling the system allows for tuning the broadband transmission to any incident angle, even at normal incidence.

It is important to understand the role of $G^{\mathrm{I,\ III}}$ in the mechanism of broadband transmission, which accounts for the acoustic coupling between the fundamental eigenmode inside the hole and all the diffractive waves in each semi-infinite (reflection or transmission) space. On the one hand, for subwavelength apertures, $\lambda > L \gg a, r$, diffraction effects can be neglected as a first approximation, so the effective impedances in the reflection G^{I}, and transmission regions G^{III} (equations (A.8) and (A.9) in appendix), reduce to

$$\begin{aligned} \left|G^{\mathrm{I}}\right| &\approx \frac{F\zeta_1}{\sqrt{1-\sin^2(\theta)}} \\ \left|G^{\mathrm{III}}\right| &\approx \frac{F\zeta_3}{\sqrt{1-(c_3/c_1)^2\sin^2(\theta)}}, \end{aligned} \tag{2}$$

where we have defined $\zeta_j = \rho_j c_j$ with $j = 1$, 2 or 3 labeling regions I, II, and III, respectively. On the other hand, the impedance of the hole (relative to that of medium I) is defined as $Z = \zeta_2/\zeta_1$. Since the broadband transmission results from an impedance matching phenomenon, the presence of three dissimilar fluids in the system (in regions I, II, and III) will provide two conditions for impedance matching (i.e., $\left|G^{\mathrm{I}}\right| = Z$ and $\left|G^{\mathrm{III}}\right| = Z$), and therefore, two Brewster-like angles

$$\begin{aligned} \sin\left(\theta_{\mathrm{B}}\right) &= \sqrt{1-\left(\frac{F\zeta_1}{\zeta_2}\right)^2} \\ \sin\left(\theta_{\mathrm{B}}^{\mathrm{III}}\right) &= \frac{c_1}{c_3}\sqrt{1-\left(\frac{F\zeta_3}{\zeta_2}\right)^2}. \end{aligned} \tag{3}$$

2.2. Symmetric system ($c_1 = c_3 = c$ and $\rho_1 = \rho_3 = \rho$)

Let us first analyze the behavior of the transmittance in a symmetric system, i.e., a 'sandwich' configuration such that fluids in regions I and III are the same (with $c_1 = c_3 = c$, and $\rho_1 = \rho_3 = \rho$) but $c, \rho \neq c_2, \rho_2$. Figure 3 shows angular transmission spectra for a hole array with squares of different sizes (as indicated in the figure). Water is considered in regions I and III (with $\rho = 1000\,\mathrm{kg\,m^{-3}}$ and $c = 1470\,\mathrm{m\,s^{-1}}$), and the apertures are filled with silicon oil ($\rho_2 = 818\,\mathrm{kg\,m^{-3}}$ and $c_2 = 960\,\mathrm{m\,s^{-1}}$). In each panel, the prediction of θ_{B} by equation (3) is shown with dashed lines. The set of geometrical parameters and fluids are considered in order to provide $T = 1$ at small incident angle values, reaching even maximum transmission at $\theta = 0°$ (panel (a)). Note also that the system in panel (a) is 'invisible' for sound, for both a wide range of incident angles and wavelengths. Similar results (not shown here) are also obtained when the holes are filled with methanol, ethylether, or isopentane, and also when the porosity (total hole area) is less than 0.25%. All previous results can be understood as an impedance matching phenomenon where $\zeta < \zeta_2$ will provide a matching condition occurring at large incident angles, while for $\zeta > \zeta_2$, impedance matching brings small θ values. For experimental development, we expect that the inclusion of thin membranes to prevent fluid mixing, and the effects of fluid

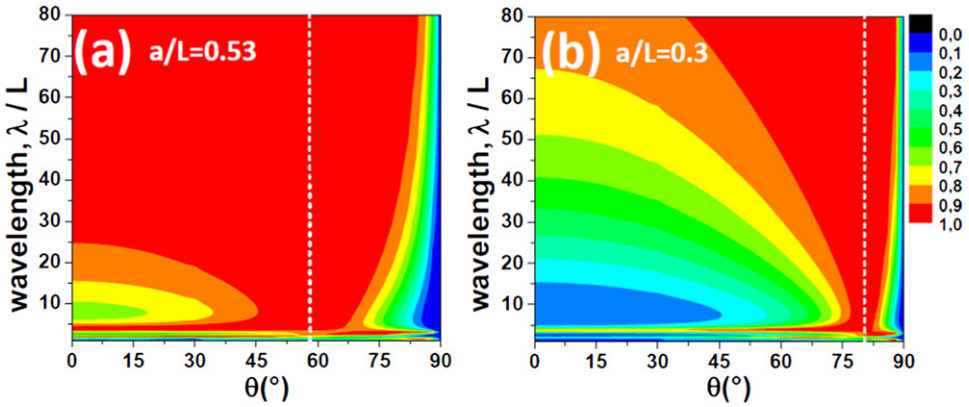

Figure 3. Angular transmission spectra for an array of square holes with (a) $a/L = 0.53$ and (b) $a/L = 0.3$, with $h/L = 1.0$, in a water–silicon–oil–water configuration (i.e., $\rho = 1000\,\mathrm{kg\,m^{-3}}$, $c = 1470\,\mathrm{m\,s^{-1}}$, $\rho_2 = 818\,\mathrm{kg\,m^{-3}}$ and $c_2 = 960\,\mathrm{m\,s^{-1}}$). Vertical dashed lines correspond to (a) $\theta_B = 58.3°$ and (b) $\theta_B = 80.3°$. The incident wavelength is defined in medium I.

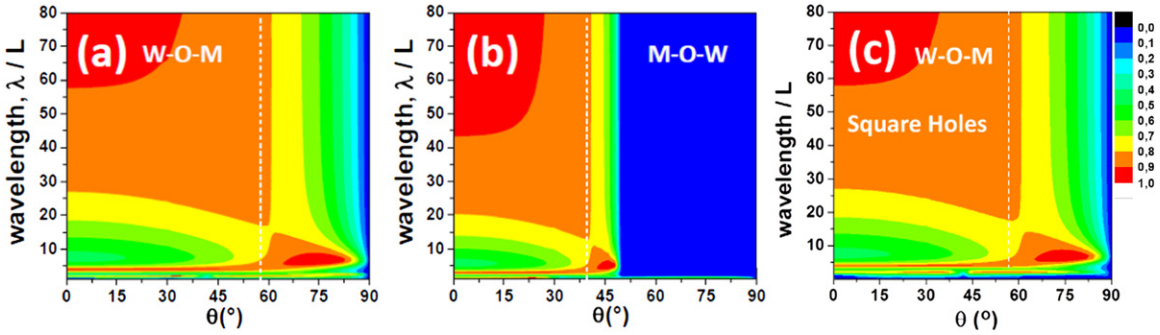

Figure 4. Angular transmission spectra for an array of circular holes with $r/L = 0.3$ and $h/L = 1.0$, considering a (a) water–silicon–oil–methanol (WOM) configuration (i.e., $\rho_1 = 1000\,\mathrm{kg\,m^{-3}}$, $c_1 = 1470\,\mathrm{m\,s^{-1}}$, $\rho_2 = 818\,\mathrm{kg\,m^{-3}}$, $c_2 = 960\,\mathrm{m\,s^{-1}}$ and $\rho_3 = 791\,\mathrm{kg\,m^{-3}}$, $c_3 = 1103\,\mathrm{m\,s^{-1}}$), (b) the inverse configuration, methanol–silicon–oil–water (MOW), and (c) for square holes in a WOM configuration with $a/L = 0.53$ (same hole area as in panel (a)) and $h/L = 1.0$. Vertical dashed lines correspond to (a) $\theta_B = 58.0°$, (b) $\theta_B^{III} = 39.5°$, and (c) $\theta_B = 58.3°$. The incident wavelength is defined in medium I.

viscosity will not strongly affect these results. Any resonances associated with the thin membranes could be tuned out of the region of interest by appropriate tensioning.

2.3. Asymmetric system ($\rho_1 \neq \rho_2 \neq \rho_3$ and $c_1 \neq c_2 \neq c_3$)

For asymmetric configurations, with different fluids in regions I, II and III (i.e., $\rho_1 \neq \rho_2 \neq \rho_3$ and $c_1 \neq c_2 \neq c_3$), the two Brewster-like angles given by equation (3) must be taken into account. In figure 4 we now consider arrays of holes of different shape, circular apertures of radius $r/L = 0.3$ (panels (a) and (b)), revealing the same bands of maximum transmission as before. For comparison, in panel (c) we also show transmission through square holes of the same area ($a/L = 0.53$) as the circles. The film thickness is $h/L = 1.0$, and we take different

fluid combinations: (a) and (c) water–silicon–oil–methanol (WOM), and (b) the inverse configuration, i.e., methanol–silicon–oil–water (MOW) (the density of methanol is $872\,\mathrm{kg\,m^{-3}}$, and the speed of sound $1103\,\mathrm{m\,s^{-1}}$). In order to have two bands of maximum transmission it must be satisfied that $0 \leqslant \sin(\theta_\mathrm{B}) \leqslant 1$ (and the same for $\theta_\mathrm{B}^\mathrm{III}$), and for some set of parameters these conditions may be not satisfied. Additionally, in order to have propagative waves in region III, the impedance (which only depends on the incident angle) $Z_{k^0}^\mathrm{III} = \zeta_3(1 - (c_3/c_1)^2\sin^2(\theta))^{-1/2}$ must be real, i.e., $\sin(\theta) < c_1/c_3$ must be fulfilled. For the WOM configuration in panels (a) and (c), only $0 \leqslant \sin(\theta_\mathrm{B}) \leqslant 1$ is satisfied, providing a single band of maximum transmission at $\theta_\mathrm{B} = 58.0°$. On the other hand, for the MOW configuration considered in panel (b), the incident wave cannot couple to propagating modes in region III for $\theta > c_1/c_3 = 48.6°$. As for those parameters, the impedance matching conditions occur for $\theta_\mathrm{B} = 71.7°$ and $\theta_\mathrm{B}^\mathrm{III} = 39.5°$, only the latter provides a broadband of maximum transmission. Note that square holes in panel (c) present maximum transmission at the corresponding Brewster angle, supporting our conclusions that this non-resonant phenomenon is valid irrespective of the hole shape.

3. Maximum transmission

One fundamental difference between symmetric and asymmetric configurations relies on the maximum transmission, T_R. As it was previously demonstrated [4], maximum transmission in subwavelength apertures in homogeneous configurations is given by $T_\mathrm{R} = \left|I_0\right|^2 \big/ 4G_\mathrm{i}$, where G_i is the imaginary part of G (see definitions in the appendix). Finally we extend this previous work to the general case of asymmetric systems, and we provide analytical expressions for T_R as a function of the filling factor and fluid properties. The maximum transmittance is obtained following a previous work for EM waves in subwavelength holes for any dielectric environment [13]. In both the EM and acoustic cases we are solving the wave equation, and boundary conditions imposed to the electric (E) and magnetic (H) fields are analogous to those imposed to the pressure (p) and normal component of the velocity (v_z), respectively. Therefore, by solving the sound wave equation and applying some approximations (see appendix for further details), we find for acoustic waves that maximum transmittance is given by

$$T_\mathrm{R} \approx \frac{\left|I_0\right|^2}{4Z_{k^0}^\mathrm{I}} \frac{G_\mathrm{i}^\mathrm{III}}{\left|G_\mathrm{i}^+\right|^2} \tag{4}$$

with $Z_{k^0}^\mathrm{I} = (1 - \sin^2(\theta))^{-1/2}$ and $G^+ = \left(G^\mathrm{I} + G^\mathrm{III}\right)\big/2$.

In order to obtain the maximum transmission at the Brewster-like angle (either θ_B or $\theta_\mathrm{B}^\mathrm{III}$), it is convenient to define $\zeta_< = \min[\zeta_1, \zeta_3]$ and $\zeta_> = \max[\zeta_1, \zeta_3]$. Applying, first, equation (2) to equation (4), and then including the corresponding expressions for the angle (either θ_B or $\theta_\mathrm{B}^\mathrm{III}$) in equation (3) we obtain

$$T_\mathrm{R}^{\theta_\mathrm{B}} \approx \frac{4\left(\zeta_1\zeta_3\right)^2 QR}{\left(\zeta_> Q + \zeta_< R\right)^2} \tag{5}$$

with $Q = F^2\zeta_<\big/\zeta_2$ and $R = (1 + (\zeta_</\zeta_>)^2(Q^2 - 1))^{1/2}$. This equation provides maximum transmission at the Brewster-like angle and it only depends on the filling factor and fluid properties in each medium.

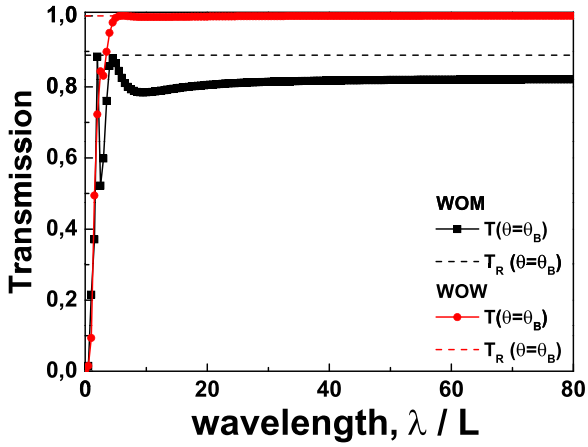

Figure 5. Transmission spectra evaluated at θ_B for a hole array with circular apertures of $r/L = 0.3$ and $h/L = 1.0$, considering either an asymmetric water–silicon–oil–methanol (WOM) system or a symmetric (WOW) one. Symbols correspond to calculations using equation (1), and discontinuous lines to equation (5).

Figure 5 shows transmission spectra for circular holes of $r/L = 0.3$ and $h/L = 1.0$ in an asymmetric (WOM) configuration, or a symmetric (WOW) system, evaluated at θ_B using transmission expressions given by equation (1) (symbol lines) or equation (5) (dashed lines). The agreement between the values of maximum transmission confirms the validity of the approximate analytical results. The estimation of maximum transmission is excellent for the symmetric (WOW) case ($T_R = 1$), and it provides a good estimation in the asymmetric (WOM) case. Note that the analytical expression only depends on the filling factor and fluid properties, and it provides an estimation with an error less than 10%.

4. Conclusions

In conclusion, we have shown that arrays of 2D subwavelength apertures in the general case when any fluid filling the system is considered, present an ultrabroadband of total transmission of acoustic waves at specific incident angles. By considering different fluids in the system, we have shown that total transmission can be tuned to any incident angle, finding even maximum transmission in a wide range of incident angles and wavelengths at the same time. We have provided analytical expressions based on the perfect rigid (PR) approximation of general application for the specific incident angle, and also for the maximum intensity at this angle.

Acknowledgments

We thank Professor F J García-Vidal of the Universidad Autónoma de Madrid, Professor J R Sambles and Dr I R Summers of the University of Exeter, for useful discussions. Financial support from the Spanish Ministry of Science and Innovation (the projects MAT2011-28581-C02 and CSD2007-046-Nanolight.es) is acknowledged. ARJM thanks Sonardyne International for financial support of his PhD.

Appendix

The linearized Euler's equations describe acoustic waves of small disturbances in fluids, and in the absence of viscosity they read

$$\begin{aligned} \nabla \mathbf{v} - \frac{\mathrm{i}\omega}{c^2\rho} p = 0, \\ \nabla p - \mathrm{i}\omega\rho\mathbf{v} = 0 \end{aligned} \tag{A.1}$$

with p, $\mathbf{v}$, c and ρ the variation in pressure, particle velocity, speed of sound, and density, respectively, due to the presence of a low-amplitude acoustic field in the medium. In the above equations $p = c^2\rho$ has been considered.

The system under study consists of a perfectly rigid (PR) film with holes on it and periodically arranged in a rectangular lattice. The geometrical parameters defining the film are the thickness h (located at $z = 0$ and $z = h$), and the array period L (along the x- and y-axes). The whole space is divided into three regions: the reflection region I, ($z < 0$), the transmission region III, ($z > h$), and the holey-screen region II. The fluid in each region is defined by its density (ρ) and speed of sound (c), and in the following we will use subscripts 1, 2, and 3 accordingly to regions I, II, and III, respectively.

The theoretical formalism used throughout this paper is based on a modal expansion of the pressure and velocity fields in the different regions. We assume that the incident acoustic field is a plane wave coming from region I. The acoustic fields in this region can be expressed as an incident plane wave $|\mathbf{k}_\parallel^0\rangle$, plus a sum of the reflected Bloch waves $|\mathbf{k}_\parallel\rangle$ weighed with their corresponding reflection coefficients, $r_\mathbf{k}$

$$\begin{aligned} \left|p^{\mathrm{I}}\right\rangle &= Z_{k^0}^{\mathrm{I}} \left|\mathbf{k}_\parallel^0\right\rangle \mathrm{e}^{\mathrm{i}k_{z1}^0 z} + \sum_{\mathbf{k}} r_\mathbf{k} Z_\mathbf{k}^{\mathrm{I}} \left|\mathbf{k}_\parallel\right\rangle \mathrm{e}^{-\mathrm{i}k_{z1}z} \\ \left|v_z^{\mathrm{I}}\right\rangle &= \left|\mathbf{k}_\parallel^0\right\rangle \mathrm{e}^{\mathrm{i}k_{z1}^0 z} - \sum_{\mathbf{k}} r_\mathbf{k} \left|\mathbf{k}_\parallel\right\rangle \mathrm{e}^{-\mathrm{i}k_{z1}z}. \end{aligned} \tag{A.2}$$

In the above expressions, $Z_\mathbf{k}^{\mathrm{I}} = k_0/k_{z1}$ is the impedance relating pressure and velocity. In this region the fields are expressed in terms of real space Bloch waves

$$\left\langle \boldsymbol{r}_\parallel \middle| \boldsymbol{k}_\parallel \right\rangle = \frac{\mathrm{e}^{\mathrm{i}\boldsymbol{k}_\parallel \boldsymbol{r}_\parallel}}{L} \tag{A.3}$$

with $\boldsymbol{r}_\parallel = (x, y)$ and the parallel momentum associated with Bloch modes $\mathbf{k}_\parallel^2 = k_x^2 + k_y^2$ with discrete diffraction orders n_x and n_y (n_x, $n_y = -\infty,..\,0\,..,\infty$) comprising in-plane scattering, where $k_x = k_x^0 + 2\pi n_x/L$, and $k_y = k_y^0 + 2\pi n_y/L$. Hence the z-component of the wave vector is $k_{z1} = (k_0^2 - \mathbf{k}_\parallel^2)^{1/2}$, where $k_0 = 2\pi/\lambda$. Finally, we define the angle of incidence with respect to the normal of the surface, θ, like $k_y^0 = k_0 \sin(\theta)$. Typically, taking diffraction orders $n_x \in (-10, 10)$ and $n_y \in (-10, 10)$, provides results with an error <0.1%.

In the same way, the fields in region III are expanded into plane waves and weighed with their corresponding transmission coefficients, $t_\mathbf{k}$

$$\begin{aligned}\left|p^{\mathrm{III}}\right\rangle &= \sum_{\mathbf{k}} t_{\mathbf{k}} Z_{\mathbf{k}}^{\mathrm{III}} \left|\mathbf{k}_{\parallel}\right\rangle \mathrm{e}^{-\mathrm{i}k_{z3}(z-h)},\\ \left|v_z^{\mathrm{III}}\right\rangle &= \sum_{\mathbf{k}} t_{\mathbf{k}} \left|\mathbf{k}_{\parallel}\right\rangle \mathrm{e}^{-\mathrm{i}k_{z3}(z-h)}.\end{aligned} \tag{A.4}$$

Now, the pressure and velocity fields are related through $Z_{\mathbf{k}}^{\mathrm{III}} = \rho_3 k_0 / (\rho_1 k_{z3})$, with $k_{z3} = ((c_1/c_3 k_0)^2 - \mathbf{k}_{\parallel}^2)^{1/2}$.

Within the PR approximation, the modes inside the apertures coincide with the waveguide modes of those apertures (which are known analytically for some geometries [4, 6, 14]). In the case of subwavelength holes, considering only the first eigenmode ($|0\rangle$) inside the apertures provides a good approximation for the total transmittance. We express the pressure and velocity field in region II as

$$\begin{aligned}\left|p^{\mathrm{II}}\right\rangle &= Z\left(A\mathrm{e}^{\mathrm{i}q_z z} + B\mathrm{e}^{-\mathrm{i}q_z z}\right)|0\rangle,\\ \left|v_z^{\mathrm{II}}\right\rangle &= \left(A\mathrm{e}^{\mathrm{i}q_z z} - B\mathrm{e}^{-\mathrm{i}q_z z}\right)|0\rangle.\end{aligned} \tag{A.5}$$

The z-component of the wave vector of the fundamental mode is $q_z = c_1/c_2 k_0$, and $Z = \rho_2 k_0/(\rho_1 q_z)$. A and B are unknown expansion coefficients that can be calculated imposing appropriate boundary conditions to the acoustic fields at the interfaces of the system ($z = 0$ and $z = h$). The normal component of the velocity v_z is continuous everywhere along the I-II and II-III interfaces, but the pressure p is continuous only at the openings.

$$\begin{cases}\displaystyle\sum_{\mathbf{k}} Z_{\mathbf{k}}^{\mathrm{I}} \left|S_{\mathbf{k}}\right|^2 (A - B) + Z(A + B) &= 2Z_{k^0}^{\mathrm{I}} S_{k^0},\\ \displaystyle\sum_{\mathbf{k}} Z_{\mathbf{k}}^{\mathrm{III}} \left(A\mathrm{e}^{\mathrm{i}q_z z} - B\mathrm{e}^{-\mathrm{i}q_z z}\right) \left|S_{\mathbf{k}}\right|^2 &= Z\left(A\mathrm{e}^{\mathrm{i}q_z z} + B\mathrm{e}^{-\mathrm{i}q_z z}\right).\end{cases} \tag{A.6}$$

We now define $v = (A - B)$ and $v' = -(A\mathrm{e}^{\mathrm{i}q_z z} - B\mathrm{e}^{-\mathrm{i}q_z z})$, and substitute in the above equations to obtain

$$\begin{cases}\left(G^{\mathrm{I}} - \Sigma\right) v - G_\nu v' &= I_0,\\ \left(G^{\mathrm{III}} - \Sigma\right) v' - G_\nu v &= 0,\end{cases} \tag{A.7}$$

with

$$\begin{cases} I_0 = 2\mathrm{i} S_{k_0} Z_{k^0}^{\mathrm{I}},\\ G_\nu = Z / \sin\left(q_z h\right),\\ \Sigma = Z \cos\left(q_z h\right) / \sin\left(q_z h\right),\\ G^{\mathrm{I,III}} = \displaystyle\sum_{\mathbf{k}} Z_{\mathbf{k}}^{\mathrm{I,\,III}} \left|S_{\mathbf{k}}\right|^2. \end{cases} \tag{A.8}$$

In the above expressions, $S_{\mathbf{k}}$ is the overlap between plane waves and the fundamental mode inside the apertures ($|\langle 0|$), which for hole arrays takes the form $S_{\mathbf{k}} = \langle \mathbf{k}|0\rangle = \int \left\langle \mathbf{k}|\boldsymbol{r}_{\parallel}\right\rangle \left\langle \boldsymbol{r}_{\parallel}|0\right\rangle \mathrm{d}\boldsymbol{r}_{\parallel}$. For square apertures (of side a) and circular holes (of radius r), the general expressions of the overlap with the first eigenmode inside the apertures are the

following

$$S_{\mathbf{k}} = \frac{a}{L}\,\mathrm{sinc}\left(\frac{k_x a}{2}\right)\mathrm{sinc}\left(\frac{k_y a}{2}\right);\ \text{for square holes},$$

$$S_{\mathbf{k}} = \frac{2\sqrt{\pi}}{L}\frac{J_1\left(k_{\parallel} r\right)}{k_{\parallel}};\ \text{for circular holes}, \tag{A.9}$$

where, $\mathrm{sinc}(x) = \sin(x)/x$, and $J_1(x)$ is the Bessel function of 1st order.

By solving the system of equations in equation (A.7), and thus knowing the modal velocities v and v', an entire field mapping can be obtained comprising far-field and near-field distributions.

Finally, in order to know the transmittance of sound at the other side of the screen, we calculate the ratio between the transmitted acoustic power and the incident one by integrating the time-averaged x-component of the acoustic intensity in each region within one unit cell, $I = \int \mathrm{Re}\,\langle x \mid p\rangle \langle x \mid v_z\rangle \mathrm{d}x$. Transmission can be defined in a plane inside the apertures (T_{II}), or in a plane in region III (T_{III}), and it can be written in terms of the previous objects as

$$T_{\mathrm{II}} = \frac{1}{Z^{\mathrm{I}}_{k^0}} G_\nu\ v\ v'^{*},$$

$$T_{\mathrm{III}} = \frac{1}{Z^{\mathrm{I}}_{k^0}} G^{\mathrm{III}} v'\ v'^{*}. \tag{A.10}$$

with * accounting for complex conjugate. These expressions are especially useful since in the rigid approach there are no absorption losses and therefore, the law of conservation of energy entails $T_{\mathrm{II}} = T_{\mathrm{III}}$.

In order to obtain equation (5), we can solve equation (A.7) again and apply that $G^- \gg G^+$ to obtain

$$T \approx \frac{\left|I_0\right|^2}{Z^{\mathrm{I}}_{k^0}} \frac{G_i^{\mathrm{III}} \left|G_\nu\right|^2}{\left[\left|G^+ - \Sigma\right|^2 - \left|G_\nu\right|^2\right]^2 + 4\left(G_i^+\right)^2 \left|G_\nu\right|^2}. \tag{A.11}$$

Taking the limit $q_z h \to 0$ in the expressions of G_ν and Σ in equation (A.8), which is a valid approximation when $\lambda \gg h$, it is possible to get equation (5) after some algebra.

References

[1] Ebbesen T W, Lezec H L, Ghaemi H F, Thio T and Wolff P A 1998 *Nature* **391** 667

[2] Garcia-Vidal F J, Martin-Moreno L, Ebbesen T W and Kuipers L 2010 *Rev. Mod. Phys.* **82** 729

[3] Lu M-H, Liu X-K, Feng L, Li J, Huang C-P, Chen Y-F, Zhu Y-Y, Zhu S-N and Ming N-B 2007 *Phys. Rev. Lett.* **99** 174301

[4] Christensen J, Martin-Moreno L and Garcia-Vidal F J 2008 *Phys. Rev. Lett.* **101** 014301

[5] Wang X 2010 *J. Appl. Phys.* **108** 064903

[6] Estrada H, Candelas P, Uris A, Belmar F, Meseguer F and de Abajo F J G 2011 *Wave Motion* **48** 235

[7] Alú A, D'Aguanno G, Mattiucci N and Bloemer M J 2011 *Phys. Rev. Lett.* **106** 123902

[8] D'Aguanno G, Le K Q, Trimm R, Alù A, Mattiucci N, Mathias A D, Aközbek N and Bloemer M J 2012 *Sci. Rep.* **2** 340
[9] Qiu C, Hao R, Li F, Xu S and Liu Z 2012 *Appl. Phys. Lett.* **100** 191908
[10] Qi D-X, Fan R-H, Peng R-W, Huang X-R, Lu M-H, Ni X, Hu Q and Wang M 2012 *Appl. Phys. Lett.* **101** 061912
[11] Hao R, Qiu C, Ye Y, Li C, Jia H, Ke M and Liu Z 2012 *Appl. Phys. Lett.* **101** 021910
[12] Kinsler L E, Frey A R, Coppens A B and Sanders J V 2000 *Fundamentals of Acoustics* 4th edn (New York: Wiley)
[13] Carretero-Palacios S, García-Vidal F J, Martín-Moreno L and Rodrigo S G 2012 *Phys. Rev.* B **85** 035417
[14] Jun K H and Eom H J 1995 *J. Acoust. Soc. Am.* **98** 2324